J. Am. Ceram. Soc., 96 [8] 2623–2627 (2013)
DOI: 10.1111/jace.12336

journal

Niobium-Doped Titania Photocatalyst Film Prepared via a Nonaqueous Sol-Gel Method

Bhavana N. Joshi,[‡] Hyun Yoon,[‡] Maikel F. A. M. van Hest,[§] and Sam S. Yoon[‡,†]

[‡]School of Mech. Eng., Korea University Anamdong, Seongbukgu, Seoul 136-713, Korea

[§]National Renewable Energy Laboratory, Golden, Colorado 80407

Niobium-doped Titanium dioxide ($Nb:TiO_2$) transparent films were successfully deposited on glass substrates using a non-aqueous sol-gel spin coating technique. The effect of Nb concentration on the structural and photocatalytic properties of $Nb:TiO_2$ films was studied using X-ray diffraction (XRD), scanning electron microscopy (SEM), atomic force microscopy (AFM), and UV visible spectroscopy. The films with 12 at.% (atomic percent) Nb doped TiO_2 showed excellent photocatalytic activity through 97.3% degradation of methylene blue (MB) after 2 h of UV irradiation.

I. Introduction

The anatase polymorph of TiO_2 with band gap ~3.2 eV has been extensively investigated as a semiconductor material for photocatalysis applications due to its chemical inertness, abundance in nature, nontoxicity, biocompatibility, low cost, strongly oxidative nature, and manufacturability at atmospheric conditions. TiO_2 has also been used in sensor devices, self-cleaning applications, bactericidal treatment, dye-sensitized solar cells, drug delivery, and in other bio applications.[1]

Over the past few years, Nb-doped TiO_2 ($Nb:TiO_2$) has received special attention as a transparent conducting oxide (TCO) due to its electrical conductivity at room temperature. $Nb:TiO_2$ thin films were first reported by Furubayashi *et al.*,[2] using pulsed laser deposition, several other groups also studied $Nb:TiO_2$ using sputtering[3] and sol-gel spin coating[4] for TCO applications. The ionic radius of Nb^{5+} of 0.064 nm is slightly larger than Ti^{4+} of 0.0605 nm; therefore, Nb^{5+} works as an n-type dopant in TiO_2 lattice and generates additional carriers in its conduction band. Archana *et al.*[5] also reported the high electron mobility and optical transparency of $Nb–TiO_2$, giving rise to the enhancement in charge transport behavior after 2 at.% of Nb doping. Thus, these excess electrons with high mobility could assist the speedy initial reaction of the organic decomposition process, thereby enhancing the overall photocatalytic activity of the $Nb–TiO_2$ catalyst. Hence, the study of the effect of Nb doping on the photocatalytic activity of TiO_2 appears to be of interest. A literature survey shows very few reports available on $Nb:TiO_2$ thin film deposition for photocatalytic applications. Mattsson *et al.*[6] reported the $Nb:TiO_2$ thin films deposited by sol-gel for decomposition of acetone using visible light. They observed that the decomposition rate of $Nb:TiO_2$ was smaller than that of TiO_2, even if the $Nb:TiO_2$ showed higher absorption for visible light. They concluded that the formation of Nb=O clusters worked as electron-hole recombination centers, making $Nb:TiO_2$ less photocatalytically active. Archana *et al.*[7] also discussed carrier recombination centers due to lattice strain raised from the mismatch of Nb and Ti ions with the increase in Nb concentration. In their work, they deposited $Nb–TiO_2$ nanowires by electrospinning for dye synthesized solar cell application. They showed that the doping of 5 at.% Nb in TiO_2 gave a slight appearance of a rutile phase (<1%) in XRD. The increase in the current density and electron mobility was observed with an increase in Nb concentration from 2 to 5 at.%. However, they observed that the efficiency of cells was reduced due to the lower fill factor and open circuit voltage by the formation of carrier recombination centers due to lattice strain. Yao *et al.*[8] reported the preparation of >85% transparent $Nb:TiO_2$ films on glass using DC/RF magnetron co-sputtering. The best photocatalytic activity on methylene blue (MB) was observed for $Nb:TiO_2$ films annealed at 400°C under visible light irradiation. Porous $Nb:TiO_2$ microspheres were synthesized by Yang *et al.*[9] using ultrasonic spray pyrolysis. The photocatalytic activity of these $Nb:TiO_2$ microspheres was investigated on MB dye, where photocatalytic activity enhanced monotonically with an increase in Nb concentration due to the suppression of electron hole pair recombination.

This article presents the synthesis of $Nb:TiO_2$ sols using a nonaqueous sol-gel method that firstly involves the complexation of the titanium alkoxide precursor, and secondly involves an *in situ* production of water. In the nonaqueous sol-gel synthesis route, the *in situ* production of water via esterification reaction was initiated due to the addition of acetic acid solution. The advantage of this nonaqueous sol-gel method is that it yields uniform nanoparticles with crystal size in the range of only a few nanometers.[10] Thus, films were prepared by using the abovementioned sol-gel method produce transparent, adherent, homogeneous and photocatalytically active $Nb:TiO_2$ thin films with a thickness of ~250 nm by spin coating on a glass substrate. The study of the characteristics of transparent TiO_2 and $Nb:TiO_2$ thin films for photocatalysis application has been carried out. The effect of Nb concentration on the decomposition of MB under UV illumination has been investigated using MB as a model organic pollutant.

II. Experimental Procedure

(1) Preparation of Thin Films

Titanium n-butoxide (1.5 g) was used as a Ti precursor mixed with diethylene glycol (DEG 10 g) and acetic acid (1 g). Furthermore, an appropriate volume of niobium ethoxide was added to aforementioned Ti solution to dope with 3, 7, and 12 at.% of Nb. More than 12 at.% of Nb concentration gave films with cracks and bad adhesion, therefore doping was limited to 12 at.%. Undoped TiO_2 thin films are presented as 0 at.% $Nb:TiO_2$. After making the precursor, a transparent and homogeneous liquid was formed, which was aged for 24 h. Precleaned soda lime glass (SLG) slides

J. McKittrick—contributing editor

Manuscript No. 32522. Received December 21, 2012; approved March 14, 2013.
[†]Author to whom correspondence should be addressed. e-mail: skyoon@korea.ac.kr

(2 cm × 2 cm) were used as a substrate. The precursor solution of 1 ml was dropped on the substrate then spun for 30 s at 4,000 rpm using a spin coater and preannealed at 250°C on a hot plate. This process was repeated ten times to achieve a film with a thickness of ~250 nm. Finally, the films were air annealed using a two-step process in a closed furnace; in the first step, the films were annealed for 15 min at 300°C to remove the DEG effectively, and were then further annealed for 60 min at 500°C for crystallization of TiO_2.

(2) Characterization of Thin Films

The crystalline structures of pure TiO_2 and Nb:TiO_2 thin films were identified by X-ray diffraction (XRD; D/MAX-2005, Rigaku, Tokyo, Japan) with Cu$K\alpha$ (λ = 0.154 nm). Surface morphologies and cross-sectional views of the films were imaged using a scanning electron microscope (HRSEM, XL30SFEG; Philips Co., Amsterdam, Holland). A noncontact mode atomic force microscope (AFM; XE-100, Park Systems Corp., Suwon, Korea) was used to examine the surface morphology and roughness of the spin coated films. Optical absorption in the spectral region of 300–800 was assessed using a UV–visible spectrometer (Optizen POP Mecasys Co. Ltd., Dae-Jeon, Korea).

(3) Photocatalytic Experiments

The photocatalytic activities of prepared samples for decomposition of aqueous MB solution were studied under UVA light (λ = 365 nm, 0.6 mW/cm^2). MB solution (#M2661, 0.1 wt% solution in water, Samchun Chemical, Suncheon, Korea) was mixed with deionized water at a 1:200 volume ratio (5 ppm). The aforementioned aqueous MB of about 1.5 ml was evenly poured onto the prepared films before being UVA irradiated. In addition, the MB solution was collected at different time intervals and changes in concentrations were estimated by measuring the intensity of the MB absorption peak at 664 nm using the UV–visible spectrometer.[11] Tests were repeated to confirm the reliability of the results.

III. Results and Discussion

The viscosity of sols was measured before thin film deposition using a LVDV-I+CP viscometer (Brookfield). The average viscosity of Nb:TiO_2 sols with Nb concentrations of 0, 3, 7, and 12 at.% was 28.7, 30.5, 33.3, and 35.2 cP, respectively. The increase in viscosity was due to the increase in Nb ethoxide concentration.

The X-ray diffraction patterns of TiO_2 and Nb:TiO_2 films with different Nb concentrations are shown in Fig. 1(a). The anatase phase in all films is confirmed by peaks at 2θ = 24.9°, 37.42°, 47.56°, 53.34°, and 54.56° corresponding to the (101), (004), (200), (105), and (211) orientation planes, respectively, which is in agreement with JCPDS card 21-1272. A literature survey shows that the formation of rutile phase depends on deposition method, crystal size, and other processing parameters.[12] Archana *et al.*[5] and Yang *et al.*[9] observed a slight trace of the rutile phase in XRD with (110) peak at 2θ ~ 27.5°. However, in our case, rutile phase peaks related to TiO_2 or Nb_2O_5 were not observed in Nb–TiO_2 films, and this concurs with the results from previous studies,[13–15] which implies the incorporation of $Nb5^+$ into the TiO_2 lattice. The lattice constant calculated using the formulations given by Ghazzal *et al.*[16] is plotted as a function of the Nb concentration shown in Fig. 1(b). Although the lattice constant *a* proportionally increases with Nb concentration, no dependence of lattice constant *c* was observed. The increase in a single lattice constant indicates that the films have tensile stress. The strain (ε) effect and residual stress (σ)[16] on the lattice constants that have been calculated from the lattice spacing of anatase films for (101) and (004) orientations are presented in Table I. The crystal

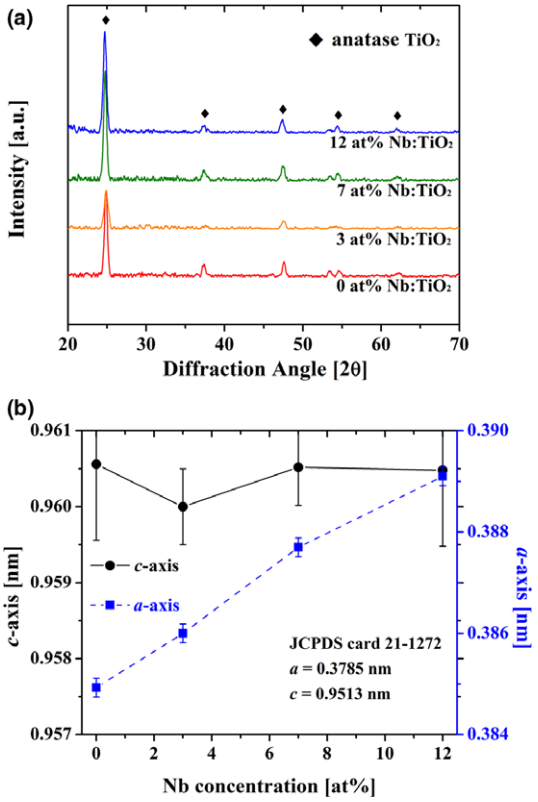

Fig. 1. (a) XRD spectra of Nb:TiO_2 thin films, (b) Effect of Nb concentration on lattice constant of Nb:TiO_2 thin films.

Table I. Comparison of Lattice Constant, Strain, Stress, and Crystal Size Determined from XRD

	Strain (10^{-3})		Stress (GPa)	
Sample	$\varepsilon_{(101)}$	$\varepsilon_{(004)}$	$\sigma_{(101)}$	$\sigma_{(004)}$
JCPDS (21-1272)	0	0	0	0
0 at.% Nb:TiO_2	−15.1	−9.84	−7.48	−4.88
3 at.% Nb:TiO_2	−16.7	−9.25	−8.27	−4.59
7 at.% Nb:TiO_2	−21.5	−9.8	−10.6	−4.86
12 at.% Nb:TiO_2	−24.7	−9.76	−12.3	−4.84

size calculated by Scherrer's formula decreased slightly from 19.8 to 18.6 nm with increasing Nb concentration. The (101) orientation peak at 25.28° mentioned in JCPDS card 21-1272 was slightly shifted to the lower 2θ (24.9°) for pure TiO_2. This shift could be attributed to the formation of stress, as shown in Table I. The incorporation of higher ionic radius Nb^{5+} ion into the TiO_2 crystal lattice results in a shift of the anatase (101) peak to a lower value compared to pure TiO_2.

The first row in Fig. 2 shows the SEM images of the surface morphology of Nb:TiO_2 thin films. The films consist of a fairly uniform granular structure. As observed in XRD, the SEM images also show the reduced grain size with increasing Nb concentration. The second row in Fig. 2 shows the 3D AFM images of Nb:TiO_2 thin films with varying Nb concentrations. The average roughness (R_a) of films that was acquired from a 2.5 μm × 2.5 μm scanned area of films is presented with each AFM image.

Figure 3 shows the transmittance spectra of the TiO_2 and Nb:TiO_2 films at room temperature. The measurements were taken at normal incidence using bare SLG substrate as a reference. The average transmittance of each film in the visible range (400–800 nm) is presented in Table II. The film's color changed from transparent pink to faint green with the increase in Nb concentration, as shown in the inset in Fig. 3. Table III shows the direct optical band gap energy of thin films obtained by plotting a square of absorption coefficient

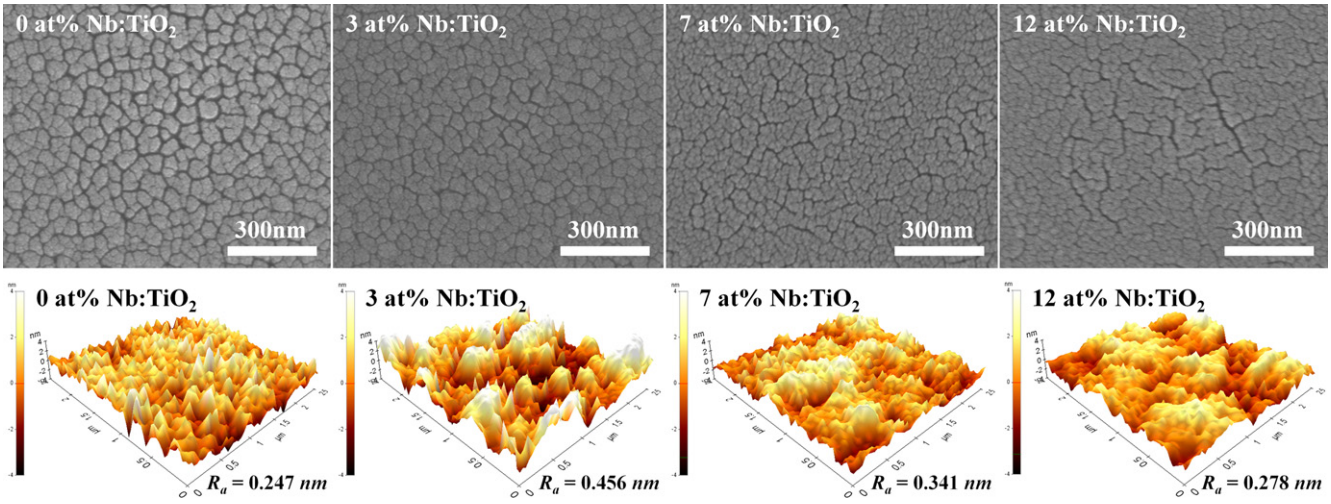

Fig. 2. The up row shows SEM surface images and bottom row presents 3D view of AFM for various Nb concentrations.

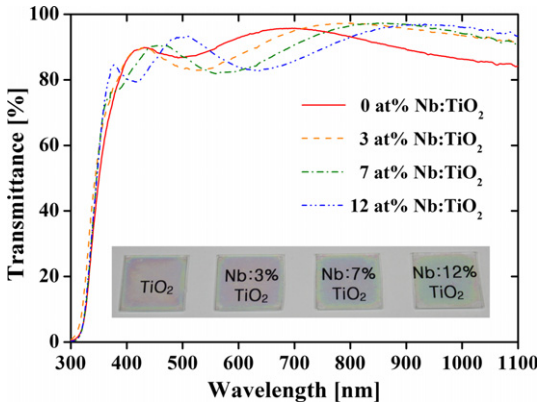

Fig. 3. UV–Visible transmittance spectra for different concentrations of Nb:TiO_2 thin films.

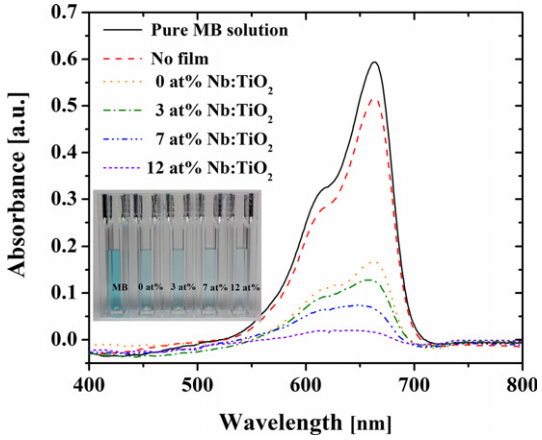

Fig. 4. Effect of Nb concentration on MB degradation after 2 h of UV illumination.

Table II. Influence of Nb Concentration on Transmittance Averaged in Visible Range ($400 < \lambda < 800$ nm) and Band Gap of Nb:TiO_2 Thin Films

Sample	Average transmittance (%)	Band gap (eV)
0 at.% Nb:TiO_2	91.08	3.84
3 at.% Nb:TiO_2	87.96	3.87
7 at.% Nb:TiO_2	86.8	3.82
12 at.% Nb:TiO_2	86.3	3.81

Table III. Reaction Parameters of Photocatalysis for Nb:TiO_2 Thin Films

Sample	k ($min^{-1} \times 10^{-3}$)	D (%)
0 at.% Nb:TiO_2	9.0	71.8
3 at.% Nb:TiO_2	10.6	78.9
7 at.% Nb:TiO_2	14.8	89.1
12 at.% Nb:TiO_2	24.3	97.3

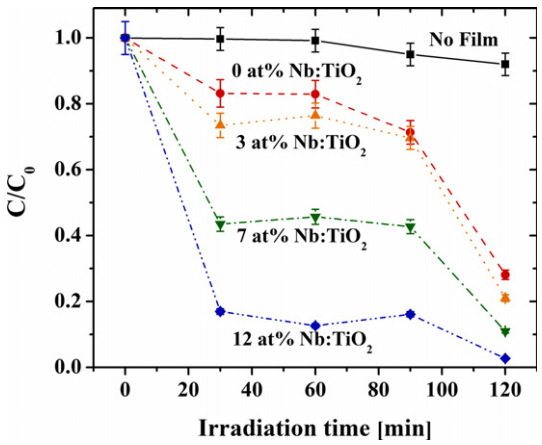

Fig. 5. Photocatalytic degradation of MB as a function of time for various Nb:TiO_2 doping concentrations.

(α^2) as a function of photon energy ($h\nu$) and by the intersection of the linear part of the curve and the horizontal axis. The band gap value for undoped TiO_2 concurs with the results found by Malengreaux *et al.*[17] for TiO_2 thin films using the nonaqueous sol-gel method using a TTIP precursor on SLG. However, after doping of Nb, the band gap variation was minimal; this could be due to the small crystal size as well as the stress formed in the crystal.

Figure 4 shows the photocatalytic activities of different concentrations of Nb:TiO_2 thin films from the decolorization of aqueous MB dye after 2 h of UVA irradiation. The presence of the characteristic absorption peak of MB at 664 nm decreased with increasing Nb concentration. The highest degradation of MB is observed for the 12 at.% Nb:TiO_2 thin film. As expected, MB degradation in the absence of a catalyst film was negligible after 2 h of UV irradiation. The inset of Fig. 4 represents the

Table IV. Comparison of Nb:TiO_2 Thin Films with Previous Photocatalysis Work

Author	Method and other paramters	Organic pollutant	Light and intensity	Irradiation time (h)	Remark
Mattsson *et al.*[6]	Sol-gel Annealing 450° for 30 min in air	Acetone	Visible light by Xenon arc lamp using AM (1.5) filter with intensity 166 mW/cm^2	0–1	Degradation of Acetone is possible by pure TiO_2 only Nb doping in TiO_2 formed Nb=O clusters which act as recombination sites lowering the photocatalytic activity
Yao *et al.*[8]	DC/RF co-sputtering annealing at 400 and 500°C for 1 h in air	MB (1.337×10^{-3} M, volume 3 ml)	Visible light bulbs (NEC, FL15EX-D-X)	0–48	Nb:TiO_2 films annealed at 400°C showed good photocatalytic activity
Yang *et al.*[9]	Ultrasonic spray pyrolysis microspheres	MB	Visible light by Xenon lamp with cutoff filter of 400 nm and output intensity 67 mW/cm^2	0–3	5 mol% Nb:TiO_2 films shows better photocatalytic activity in solar and visible light
Kaleji *et al.*[13]	Sol-gel dip coating 475°C for 1 h in air	MB concentration 5 ppm	UV lamp with 360 nm wavelength and 8 W intensity	0–2	1 mol% of Nb:TiO_2 films showed better photocatalytic activity
The present work	Nonaqueous sol-gel annealing at 500°C for 30 min in air	MB Concentration 5 ppm (1.5 ml)	UV 365 nm light with intensity 0.6 mW/cm^2	0–2	12 at.% Nb:TiO_2 films showed 97.3% MB degradation in 2 h of UV irradiation

decolorization of MB compared to the original solution. The reaction mechanism of photocatalytic decolorization of MB in the presence of Nb:TiO_2 can be explained in a similar manner as that of TiO_2, as explained in our earlier reports.[1] However, the enhancement in photocatalytic activity after Nb doping is likely due to an increase in carrier electrons from pentavalent Nb. This increase in electron concentration in Nb:TiO_2 thin films consequently gives a faster reaction by forming more superoxide radicals. The formed hydroxyl and superoxide radicals react with MB to yield degradation products such as CO_2, NO_3, NH_4^+, and SO_4^{-2}. Thus, the final reaction can be represented in the following way:

$$\mathrm{MB} + \mathrm{Nb:TiO_2} \xrightarrow{h\nu(\mathrm{UVA})} \mathrm{CO_2} + \mathrm{H_2O} + \mathrm{NO_3} + \mathrm{NH_4^+} + \mathrm{SO_4^{-2}} + \mathrm{Nb:TiO_2}$$

The time dependency of C/C_0 under UV irradiation using Nb:TiO_2 thin films for different Nb concentrations is shown in Fig. 5 where C is the concentration of MB after different irradiation time (t in min) and C_0 is the initial MB concentration. The photocatalytic degradation of MB solution by Nb:TiO_2 thin films under UV irradiation can be modeled using the Langmuir–Hinshelwood (LH)[18] reaction kinetics. For low concentration MB solution the LH reaction can be expressed in terms of a pseudo first-order reaction $\ln(C_0/C) = kt$ and the apparent reaction rate constant 'k' can be obtained from the fitted straight line plots of $\ln(C_0/C)$ versus t. Table III clearly reveals that the apparent reaction rate constant 'k' and degradation efficiency 'D' increases with escalation in Nb concentration. After 2 h of UV irradiation 12 at.% Nb:TiO_2 thin film exhibited highest rate constant of 24.3×10^{-3} min^{-1}, which was twice that of undoped TiO_2. As mentioned earlier, the pentavalent $Nb5^+$ ion doping in TiO_2 introduces more electrons in the conduction band and some shallow donor levels below the conduction edge. These extra electrons give more superoxide radicals consequently enhancing the photocatalytic efficiency of Nb:TiO_2 thin films.

Table IV compares the photocatalytic study of Nb:TiO_2 thin films carried out by previous studies. The transparency in our case for undoped and doped samples was greater than 86%. In addition, 97.3% of MB degradation was observed in 2 h of UVA irradiation for 12 at.% of Nb:TiO_2 thin films.

IV. Conclusions

Transparent Nb:TiO_2 thin films were deposited successfully using the nonaqueous sol-gel technique. XRD analysis confirmed the presence of only the anatase phase of TiO_2 in both the TiO_2 and Nb:TiO_2 films. The crystal size decreased with an increase in Nb concentration. The highest photodegradation efficiency of 97.3% was observed for 12 at.% Nb:TiO_2 thin films after 2 h of UV irradiation and the reaction rate was two times higher than that of undoped TiO_2.

Acknowledgments

This study was supported by a grant from the cooperative R&D Program (B551179-08-03-00) funded by Korea Research Council Industrial Science and Technology, Republic of Korea. This research was also supported by Converging Research Center Program through the Ministry of Education, Science and Technology (2010K000969), and NRF-2012029433, NRF-2012-0001169, and NRF-2012K1A3A1A09054910.

References

[1]H. Yoon, B. Joshi, S.-H. Na, and S. S. Yoon, "Antibacterial Activity and Photocatalysis of Electrosprayed Titania Films," *J. Electrochem. Soc.*, **159** [11] H823–7 (2012).

[2]Y. Furubayashi, T. Hitosugi, Y. Yamamoto, K. Inaba, G. Kinoda, Y. Hirose, T. Shimada, and T. Hasegawa, "A Transparent Metal: Nb-Doped Anatase TiO_2," *Appl. Phys. Lett.*, **86** [25] 1–3 (2005).

[3]N. Yamada, T. Hitosugi, N. L. H. Hoang, Y. Furubayashi, Y. Hirose, T. Shimada, and T. Hasegawa, "Fabrication of Low Resistivity Nb-Doped TiO_2 Transparent Conductive Polycrystalline Films on Glass by Reactive Sputtering," *Jpn. J. Appl. Phys.*, **46**, 5275–7 (2007).

[4]C. Wang, J. Meinhardt, and P. Löbmann, "Growth Mechanism of Nb-Doped TiO_2 Sol-Gel Multilayer Films Characterized by SEM and Focus/Defocus TEM," *J. Sol-Gel. Sci. Technol.*, **53** [2] 148–53 (2010).

[5]P. S. Archana, R. Jose, T. M. Jin, C. Vijila, M. M. Yusoff, and S. Ramakrishna, "Structural and Electrical Properties of Nb-Doped Anatase TiO2 Nanowires by Electrospinning," *J. Am. Ceram. Soc.*, **93** [12] 4096–102 (2010).

[6]A. Mattsson, M. Leideborg, K. Larsson, G. Westin, and L. Österlund, "Adsorption and Solar Light Decomposition of Acetone on Anatase TiO_2 and Niobium Doped TiO_2 Thin Films," *J. Phys. Chem. B*, **110** [3] 1210–20 (2006).

[7]P. S. Archana, R. Jose, M. M. Yusoff, and S. Ramakrishna, "Near Band-Edge Electron Diffusion in Electrospun Nb-Doped Anatase TiO_2 Nanofibers Probed by Electrochemical Impedance Spectroscopy," *Appl. Phys. Lett.*, **98** [15] 152103, 3pp (2011).

[8]H.-C. Yao, M.-C. Chiu, D.-C. Tsai, C.-J. Huang, and F.-S. Shieu, "Effect of Annealing on the Nb-Doped TiO_2 Films Prepared by DC/RF Cosputtering," *J. Electrochem. Soc.*, **155** [9] G173–9 (2008).

[9]J. Yang, X. Zhang, C. Wang, P. Sun, L. Wang, B. Xia, and Y. Liu, "Solar Photocatalytic Activities of Porous Nb-Doped TiO_2 Microspheres Prepared by Ultrasonic Spray Pyrolysis," *Solid State Sci*., **14** [1] 139–44 (2012).

[10]M. Niederberger and N. Pinna, *Metal Oxide Nanoparticles in Organic Solvents: Synthesis, Formation, Assembly and Application*. Springer-Verlag London Ltd., London, UK, 2009.

[11]J. Ryu, D.-S. Park, B.-D. Hahn, J.-J. Choi, W.-H. Yoon, K.-Y. Kim, and H.-S. Yun, "Photocatalytic TiO_2 Thin Films by Aerosol-Deposition: From Micron-Sized Particles to Nano-Grained Thin Film at Room Temperature," *Appl. Catal. B*, **83** [1–2] 1–7 (2008).

[12]B. Grzmil, B. Kic, and M. Rabe, "Inhibition of the Anatase-Rutile Phase Transformation With Addition of K_2O, P_2O_5, and Li_2O," *Chem. Pap*., **58** [6] 410–4 (2004).

[13]B. K. Kaleji, R. Sarraf-Mamoory, and A. Fujishima, "Influence of Nb Dopant on the Structural and Optical Properties of Nanocrystalline TiO_2 Thin Films," *Mater. Chem. Phys*., **132** [1] 210–5 (2012).

[14]J. Liu, X. Zhao, L. Duan, M. Cao, H. Sun, J. Shao, S. Chen, H. Xie, X. Chang, and C. Chen, "Influence of Annealing Process on Conductive Properties of Nb-Doped TiO_2 Polycrystalline Films Prepared by Sol-Gel Method," *Appl. Surf. Sci*., **257** [23] 10156–60 (2011).

[15]Y. Liu, J. M. Szeifert, J. M. Feckl, B. Mandlmeier, J. Rathousky, O. Hayden, D. Fattakhova-Rohlfing, and T. Bein, "Niobium-Doped Titania Nanoparticles: Synthesis and Assembly Into Mesoporous Films and Electrical Conductivity," *ACS Nano*, **4** [9] 5373–81 (2010).

[16]M. N. Ghazzal, N. Chaoui, M. Genet, E. M. Gaigneaux, and D. Robert, "Effect of Compressive Stress Inducing a Band gap Narrowing on the Photo-induced Activities of Sol-Gel TiO_2 Films," *Thin Solid Films*, **520** [3] 1147–54 (2011).

[17]C. M. Malengreaux, A. Timmermans, S. L. Pirard, S. D. Lambert, J.-P. Pirard, D. Poelman, and B. Heinrichs, "Optimized Deposition of TiO_2 Thin Films Produced by a Non-Aqueous Sol-Gel Method and Quantification of Their Photocatalytic Activity," *Chem. Eng. J*., **195–196**, 347–58 (2012).

[18]K. Gopalakrishnan, H. M. Joshi, P. Kumar, L. Panchakarla, and C. Rao, "Selectivity in the Photocatalytic Properties of the Composites of TiO_2 Nanoparticles With B-and N-Doped Graphenes," *Chem. Phys. Lett*., **511**, 304–8 (2011). □